Korean J. Chem. Eng., 37(6), 955-960 (2020)
DOI: 10.1007/s11814-020-0541-2

pISSN: 0256-1115
eISSN: 1975-7220

Gas-phase dehydration of glycerol to acrolein over different metal phosphate catalysts

Tianlin Ma*,†,‡, Jianfei Ding,‡, Xueli Liu*, Gangling Chen*, and Jiandong Zheng***

*School of Materials and Chemical Engineering, Chuzhou University, Chuzhou, Anhui 239000, China
**School of Chemistry and Chemical Engineering, Yancheng Institute of Technology, Yancheng, Jiangsu 224051, China
(*Received 16 December 2019 • accepted 13 March 2020*)

Abstract−We conducted a comparative study of gas phase dehydration of glycerol to acrolein over aluminium phosphate, iron phosphate and nickel phosphate catalysts prepared by a simple replacement reaction method (AlP, FeP and NiP). The textural properties, acid amounts, acid types, and coke contents of the samples were studied. The results showed that all metal phosphate catalysts remained in an amorphous state. The glycerol conversion was proportional to the acid amount of metal phosphate catalyst in the glycerol dehydration reaction. Higher value of B/L was more likely to produce acrolein. Among the metal phosphate catalysts, FeP showed superior performance due to its suitable textural and acid properties. After 2 h on stream, high glycerol conversion (96%), acrolein selectivity (82%) and acrolein yield (79%) were achieved on the FeP catalyst at 280 °C. The catalyst deactivation was ascribed to carbon deposition on the catalyst surface blocking the active sites during the glycerol dehydration reaction.

Keywords: Biodiesel, Glycerol, Dehydration, Acrolein, Metal Phosphate

INTRODUCTION

Biodiesel as a renewable fuel has received intensive attention world-wide [1]. It is estimated that 10 wt% of glycerol is obtained from biodiesel produced by transesterification, generating an enormous amount of glycerol, more than the market needs [2]. Glycerol can be converted into various chemical commodities through esterification, dehydration, hydrogenolysis, reforming, oxidation, and etherification reactions [3]. In recent years, many researchers have focused on designing effective catalysts for the conversion of glycerol to acrolein, which is used widely in the production of detergents, polymers, acrylic acid esters and methionine [1-9].

To date, various solid acid catalysts have been studied for the dehydration of glycerol, including metal phosphates [10,11], metal oxides [12,13], zeolites [14-16], and heteropolyacids [1,3,5-9,17]. Among these acid catalysts, metal phosphate catalysts have been widely investigated in the glycerol dehydration reaction. Deleplanque et al. [10] studied the catalytic performance of $FePO_4$ synthesized by four different methods. They found that 100% glycerol conversion and 92% acrolein yield were obtained after 5 h of reaction over iron phosphate prepared by hydrothermal method. However, the catalysts were deactivated quickly. Estevez et al. [11] reported that the mesoporous $AlPO_4$ prepared using a simple ammonia sol-gel method exhibited 23% acrolein yield at 270 °C and 1 bar pressure. Lopez-Pedrajas et al. [18] used various binary Al/M (M=Fe, V, Ca) metal phosphates in conversion of glycerol. They found that the aluminium-vanadium phosphate exhibited the highest acrolein selectivity of 62% at 280 °C. Lopez-Pedrajas et al. [19] also studied the influence of a transition metal in the precipitation medium of $AlPO_4$. The AlCoPO650 showed a maximum acrolein yield of 54%. As mentioned, aluminium phosphate showed low acrolein selectivity and iron phosphate showed high catalytic performance in the glycerol dehydration reaction. In addition, the catalysts were prepared using H_3PO_4 as raw material, and hydrophosphate might have existed in the final synthesized products, which decreased the purity of the phosphates. Among the other metal phosphates, nickel phosphate catalysts showed excellent performance in many catalytic reactions [20-22]. To the best of our knowledge, no scientific papers have been published using nickel phosphate as catalyst for the dehydration of glycerol to acrolein. Therefore, it is necessary to compare the catalytic performance of aluminium phosphate, iron phosphate and nickel phosphate catalysts in the glycerol dehydration reaction to select the most active metal phosphate catalysts.

In this work, aluminum phosphate, iron phosphate and nickel phosphate catalysts were prepared using a simple replacement reaction method and evaluated for the dehydration of glycerol to acrolein. The purpose was to find the correlation between the structures, textural properties, acid amounts, and acid types and catalytic activities of different metal phosphate catalysts during the glycerol dehydration reaction.

EXPERIMENTAL

1. Catalyst Preparation

Aluminum phosphate (Al/P=1) was prepared by a simple replacement reaction method from $Al(NO_3)_3{\cdot}9H_2O$ and $Na_3PO_4{\cdot}12H_2O$. First, 61 g of $Al(NO_3)_3{\cdot}9H_2O$ and 61.8 g of $Na_3PO_4{\cdot}12H_2O$ were added to 350 mL of deionized water in a 500 mL of round-bottom flask under stirring. The solution was stirred at 100 °C for 5 h until no more precipitate formed. After the solution was cooled, the solution was filtrated and washed with deionized water twenty times to completely remove Na species. The material was dried at 120 °C

†To whom correspondence should be addressed.
E-mail: matianlin951@sina.com
‡T. Ma and J. Ding contributed equally to this work.

for 12 h and calcined at 500 °C for 4 h in a muffle furnace at a heating rate of 5 °C/min prior to reaction. The resulting material was denoted as AlP.

Iron phosphate (Fe/P=1) was prepared by a simple replacement reaction method from $Fe(NO_3)_3{\cdot}9H_2O$ and $Na_3PO_4{\cdot}12H_2O$. First, 53.6 g of $Fe(NO_3)_3{\cdot}9H_2O$ and 50.4 g of $Na_3PO_4{\cdot}12H_2O$ were added to 350 mL of deionized water in a 500 mL of round-bottom flask under stirring. The solution was stirred at 100 °C for 5 h until no more precipitate formed. After the solution was cooled, the solution was filtrated and washed with deionized water twenty times to completely remove Na species. The material was dried at 120 °C for 12 h and calcined at 500 °C for 4 h in a muffle furnace at a heating rate of 5 °C/min prior to reaction. The resulting material was denoted as FeP.

Nickel phosphate (Ni/P=1) was prepared by a simple replacement reaction method from $Ni(NO_3)_2{\cdot}6H_2O$ and $Na_3PO_4{\cdot}12H_2O$. First, 39.18 g of $Ni(NO_3)_2{\cdot}6H_2O$ and 29.94 g of $Na_3PO_4{\cdot}12H_2O$ were added to 350 mL of deionized water in a 500 mL of round-bottom flask under stirring. The solution was stirred at 100 °C for 5 h until no more precipitate formed. After the solution was cooled, the solution was filtrated and washed with deionized water twenty times to completely remove Na species. The material was dried at 120 °C for 12 h and calcined at 500 °C for 4 h in a muffle furnace at a heating rate of 5 °C/min prior to reaction. The resulting material was denoted as NiP.

2. Catalyst Characterization

Powder X-ray diffraction (XRD) results were collected on a Shimadzu XRD-6000 instrument with Cu-Kα radiation (40 kV, and 40 mA). Data were collected in the 2θ range from 5 to 70°. N_2 adsorption-desorption isotherms were determined by a Micromeritics ASAP 2020 instrument. The samples were pretreated at 200 °C for 2 h before measurement. Temperature programmed desorption of ammonia (NH_3-TPD) was measured on a Builder PCA-1200 analyzer. A sample of 100 mg was pretreated in He (30 mL/min) at 450 °C for 1 h, and the sample was treated with NH_3 (30 mL/min) for 0.5 h after cooling to 100 °C. The sample was purged in He atmosphere until a constant TCD level was obtained. The temperature was programmed at a heating rate of 10 °C/min to 450 °C to desorb the chemically absorbed NH_3. Infrared spectroscopy (FT-IR) of pyridine adsorption experiments was analyzed by a Shimadzu FTIR-8700 spectrometer. The samples were pretreated under vacuum at 350 °C for 1 h and then exposed to purified pyridine for 30 min at room temperature. Finally, the samples were degassed at 250 °C. The number of Brønsted and Lewis acid sites was calculated by using the integral intensities of the typical bands reported by Emeis [23]. The elemental analysis of the catalyst was by means of inductively coupled plasma optical emission spectroscopy (Thermo ICP-OES 6500). Carbon deposition formed on the used sample was determined by a CHNS analyzer.

3. Catalytic Reaction

The obtained metal phosphate catalysts were evaluated in the conversion of glycerol using a continuous-flow fixed-bed reactor (8 mm i.d.) under atmospheric pressure. The catalyst (1 g) was placed between quartz wool and fixed in the middle part of the reactor. Before the catalytic tests, the catalyst was heated at 280 °C under nitrogen flow (40 mL/min) for 1 h. A 10 wt% glycerol solution was fed into the reactor by a syringe pump with 0.08 mL/min flow-rate in a N_2 flow (10 mL/min). The reaction temperature was fixed at 280 °C. After 1 h, the products and unconverted glycerol were condensed in a water-ice mixture and taken hourly for analysis. The liquid was analyzed using a gas chromatograph assembled with a capillary column (HP-INNOWAX; 60 m×0.32 mm×0.25 μm) and a flame ionization detector using methanol as an internal standard. The glycerol conversion, product selectivity and acrolein yield were defined as follows:

$$\text{Glycerolconversion (\%)} = \frac{\text{Moles of glycerol reacted}}{\text{Moles of glycerol in thefeed}} \times 100$$

$$\text{Product selectivity (\%)} = \frac{\text{Moles of carbon in a product formed}}{\text{Moles of carbon in glycerol consumed}} \times 100$$

$$\text{Acrolein yield (\%)} = \frac{\text{Glycerol conversion} \times \text{acrolein selectivity}}{100}$$

RESULTS AND DISCUSSION

1. Catalyst Characterization

The XRD patterns of the AlP, FeP and NiP samples are shown in Fig. 1. For all synthesized catalysts, the XRD patterns show only a very broad peak between 15-45°, indicating that the catalysts appear as amorphous materials. Similar XRD results were observed by Lopez-Pedrajas et al. [18] and Liu et al. [24] Chai et al. [25] reported that amorphous Nb_2O_5 catalysts exhibited higher activity and acrolein yield than the other crystallized samples. Lopez-Pedrajas et al. [18] found that the amorphous $FePO_4$ and $AlPO_4$ showed higher performance in glycerol dehydration reaction than the other highly crystalline metal phosphates.

Fig. 2 shows the N_2 adsorption-desorption isotherms of the AlP, FeP and NiP catalysts. The pore diameter distributions of the synthesized samples are illustrated in Fig. 3. The textural properties of the samples were calculated from N_2 physical adsorption-desorption measurements and results are listed in Table 1. The specific surface area of AlP, FeP and NiP was 135 m^2/g, 87 m^2/g and 125

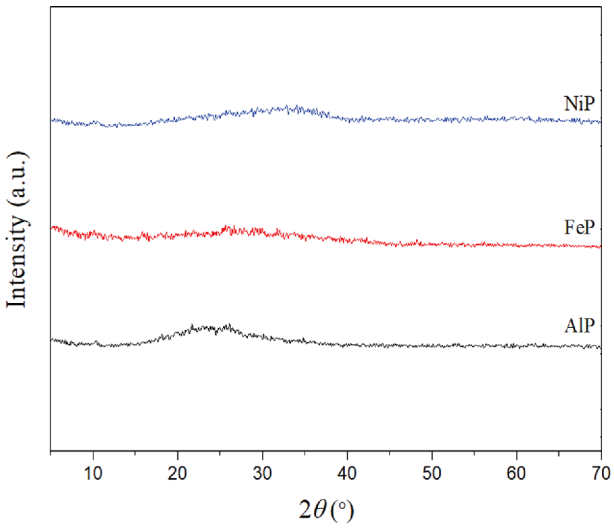

Fig. 1. XRD patterns of the AlP, FeP and NiP samples.

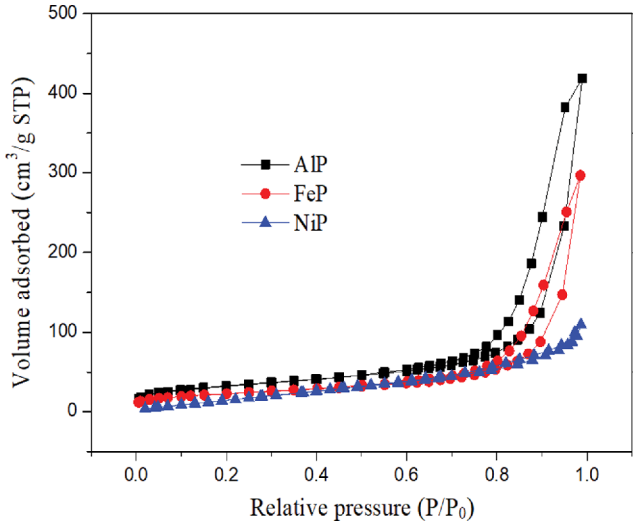

Fig. 2. Nitrogen adsorption-desorption isotherms of the AlP, FeP and NiP samples.

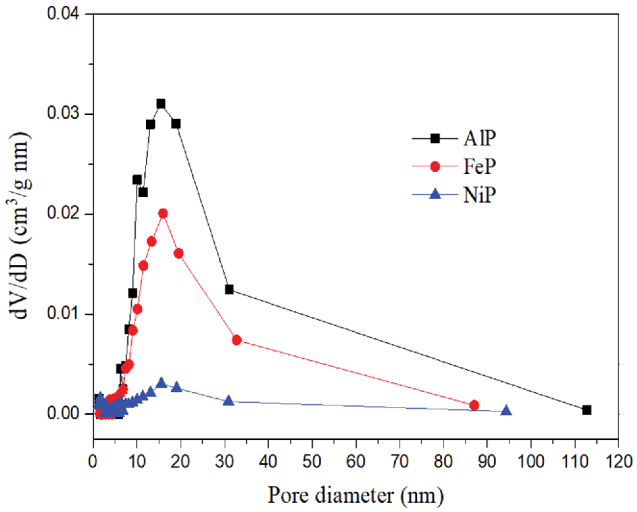

Fig. 3. Pore diameter distributions of the AlP, FeP and NiP samples.

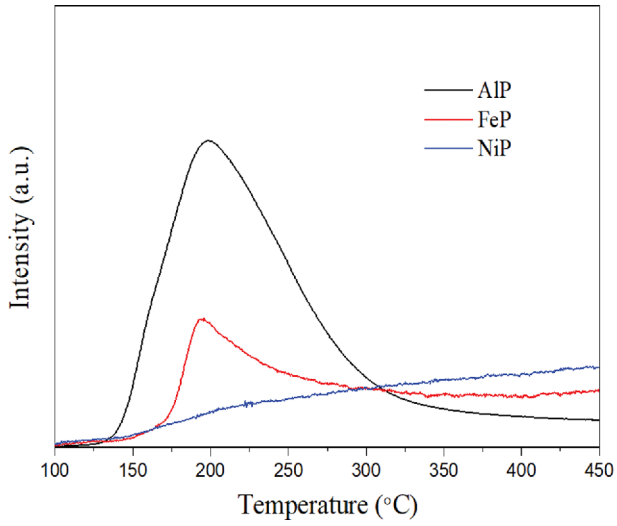

Fig. 4. NH_3-TPD profiles of the AlP, FeP and NiP samples.

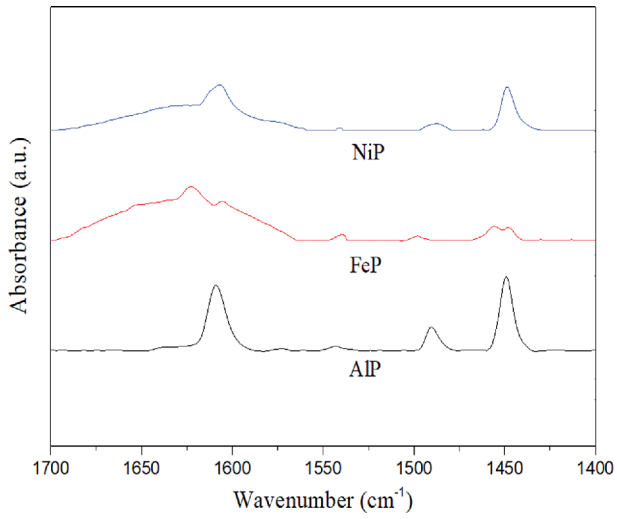

Fig. 5. Pyridine-FTIR spectra of of the AlP, FeP and NiP samples.

m^2/g, respectively. The pore volume of AlP, FeP and NiP was 0.66 cm^3/g, 0.46 cm^3/g and 0.20 cm^3/g respectively. It is noticed that FeP (16.00 nm) shows larger pore size than AlP (15.46 nm) and NiP (15.57 nm), but they do not differ significantly.

The total acid amount of catalyst measured by NH_3-TPD is an important parameter in the dehydration of glycerol to acrolein. The NH_3-TPD profiles of AlP, FeP and NiP samples are presented in Fig. 4. As can be seen, all samples present one NH_3 desorption peak centered at about 200 °C. Meanwhile, the acid amounts of the catalysts are listed in Table 1. The AlP catalyst shows the highest acid amount of 210 μmol/g, while the lowest acid amount of 42 μmol/g is achieved on NiP. According to the NH_3-TPD results, the acid amount of the metal phosphate catalyst is in the order of AlP> FeP>NiP.

In the dehydration of glycerol to acrolein, the acid type has a large influence on the product selectivities. To distinguish the acid type, pyridine-FTIR spectra were applied to determine the Brønsted and Lewis acid sites, as presented in Fig. 5. The band at about

Table 1. Textural and acidic properties of the AlP, FeP and NiP samples

Catalyst	Surface area (m^2/g)	Pore volume (cm^3/g)	Pore size (nm)	Acid amount (μmol/g)	B/L ratio
AlP	135	0.66	15.46	210	0.08
FeP	87	0.46	16.00	87	0.17
NiP	125	0.20	15.57	42	0.02

Table 2. Catalytic performance of the AlP, FeP and NiP catalysts at 280 °C and 2 h reaction time

Catalyst	X[a] (%)	Y[b] (%)	Selectivity (%)					
			Acrolein	Hydroxyacetone	Acetaldehyde	Formaldehyde	Acetic acid	Others
Blank	45	11	25	8	6	5	8	48
AlP	98	65	66	11	15	2	2	4
FeP	96	79	82	3	10	1	1	3
NiP	89	57	64	15	13	2	1	5

[a]Glycerol conversion.
[b]Acrolein yield.

1,448 cm^{-1} and 1,540 cm^{-1} corresponds to Lewis and Brønsted acid sites, respectively, and the band due to pyridine adsorbed on both Brønsted and Lewis acid sites is located at about 1,490 cm^{-1} [5,7]. It can be seen that AlP, FeP and NiP samples all possess Brønsted and Lewis acid sites. The Lewis acid sites are dominant over Brønsted acid sites. The Brønsted acid sites could be due to the surface P-OH groups, and the Al^{3+}, Fe^{3+} and Ni^{2+} are responsible for the formation of Lewis acid sites. Similar conclusions were already reached in the previous reports [11,18,26-28]. The Brønsted to Lewis acid sites ratios (B/L) are summarized in Table 1, where FeP shows the highest B/L of 0.17, while the lowest B/L of 0.02 is obtained on NiP. It is significant that many researchers reported that the Brønsted acid sites are more crucial than Lewis acid sites for the conversion of glycerol to acrolein [2,5,7-11].

2. Catalytic Activity

The catalytic results of AlP, FeP and NiP samples at 280 °C and 2 h reaction time are listed in Table 2. Acrolein is the main product over all the metal phosphate catalysts. Moreover, some byproducts including hydroxyacetone, formaldehyde, acetaldehyde and acetic acid are detected. As seen in Table 2, the glycerol conversion is 45% and acrolein selectivity is 25% under blank reaction conditions. The AlP, FeP and NiP samples exhibit higher glycerol conversion and acrolein selectivity than the blank reaction. Especially, glycerol conversion was up to >95% on AlP and FeP samples. It can be seen that the glycerol conversion is in the order of AlP>FeP>NiP, which is proportional to the acid amount of the sample. Many researchers reported that the glycerol conversion depended on the acid amount of the catalyst [8,9,29]. Acrolein selectivity and yield show an obvious difference over different metal phosphates. Among the samples, the FeP sample exhibits the highest acrolein selectivity of 82% and yield of 79%, while the NiP catalyst exhibits the lowest acrolein selectivity of 64% and yield of 57%. Fig. 6 shows the correlation between B/L ratio and acrolein yield over AlP, FeP and NiP catalysts. Note that the acrolein yield increases with increasing the B/L ratio. On the Brønsted acid sites of catalyst, protonation of glycerol was obtained at the central -OH and then the product was dehydrated to generate 3-hydroxypropanal, which was easily converted to acrolein [4,7]. The higher

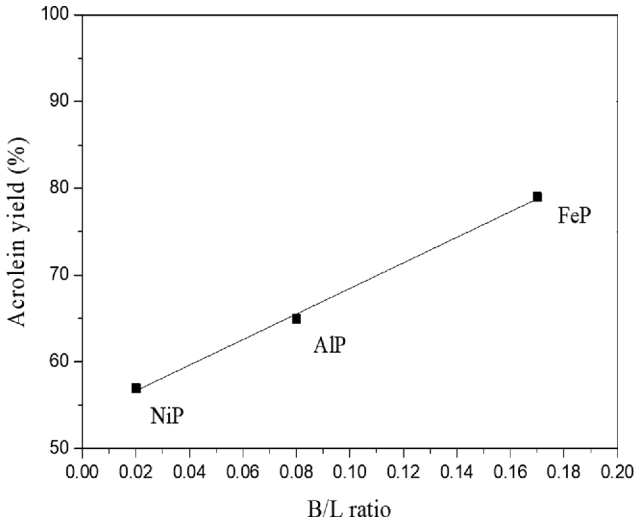

Fig. 6. Correlation between B/L ratio and acrolein yield over the AlP, FeP and NiP catalysts.

Table 3. Comparison of catalytic performance of different metal phosphate catalysts in the gas phase dehydration of glycerol to acrolein

Catalyst	Reaction temperature (°C)	Reaction time (h)	$X_{glycerol}$ (%)	$S_{acrolein}$ (%)	$Y_{acrolein}$ (%)	Refs.
Al_2O_3-PO_4	280	1	100	42	42	[29]
TiO_2-PO_4	280	1	98	37	36	[29]
$FePO_4$-H	280	5	100	92	92	[10]
Ca/HAP	350	2	85	9	7	[30]
$AlPO_4$450	280	3	41	49	20	[19]
AlCoPO450	280	3	86	51	44	[19]
AlCuPO450	280	3	77	60	46	[19]
AlP	280	2	98	66	65	This work
FeP	280	2	96	82	79	This work
NiP	280	2	89	64	57	This work

amount of Brønsted acid sites enhanced the acrolein selectivity and yield. Higher value of B/L was more likely to produce acrolein rather than hydroxyacetone [2,5,7,8].

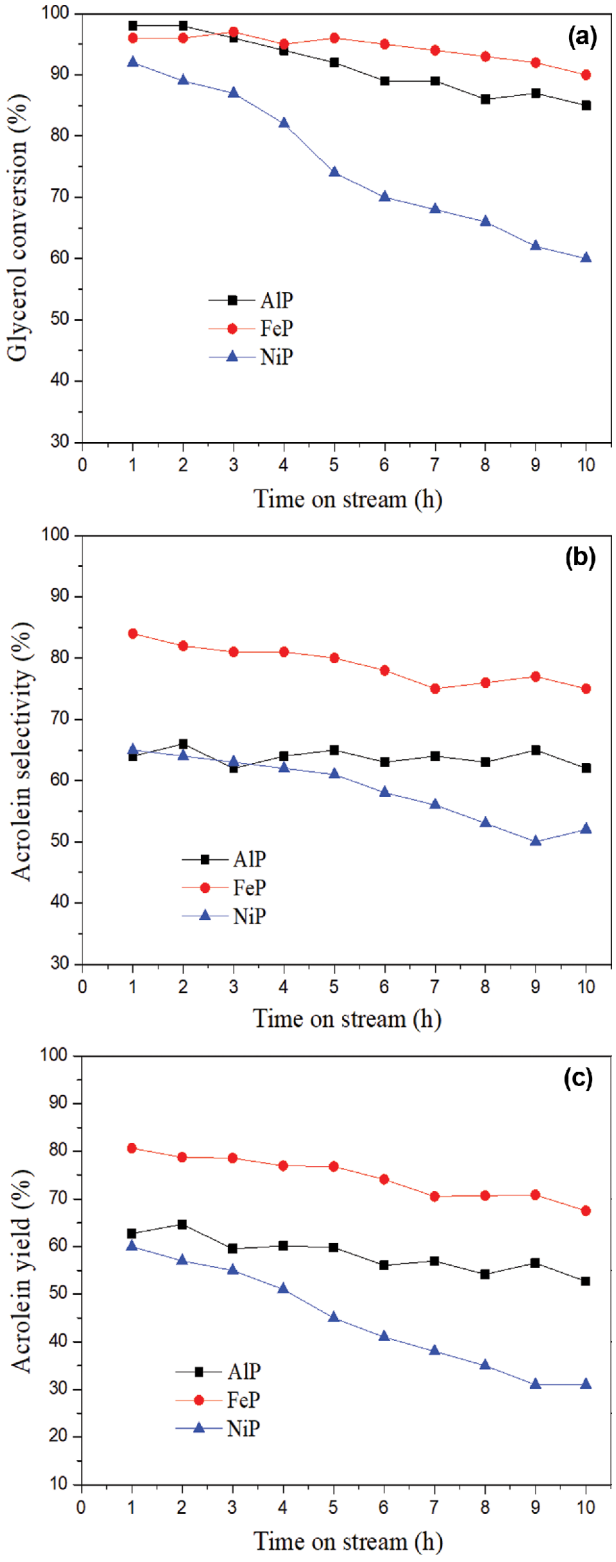

Fig. 7. (a) Glycerol conversion, (b) acrolein selectivity, and (c) acrolein yield over the AlP, FeP, and NiP samples with time on stream.

A comparison of the catalytic performance of different metal phosphate catalysts in the gas phase dehydration of glycerol to acrolein is shown in Table 3. The iron phosphate prepared by hydrothermal method shows the best catalytic performance, with 100% glycerol conversion and 92% acrolein yield after 5 h of reaction [10]. The FeP, AlP and NiP catalysts prepared by a simple replacement reaction method in this work show higher catalytic performance than other metal phosphate catalysts except for $FePO_4$-H.

The catalytic performance of AlP, FeP and NiP samples with time on stream at 280 °C is shown in Fig. 7. As shown in Fig. 7(a), the glycerol conversion over NiP is obviously lower than that over AlP and FeP catalysts during the whole reaction time. Meanwhile, the glycerol conversion over the AlP is higher than that over FeP in the first 2 h of reaction; however, after 2 h on stream the FeP always shows higher glycerol conversion than AlP. This can be because AlP with higher acid amount is more likely to be deactivated than FeP. The above results illustrate that the catalyst activity and stability are associated with the acid amount of the sample. Similar results were also reported by other researchers [8,9,29,31]. As shown in Fig. 7(b) and Fig. 7(c), the acrolein selectivity and yield of FeP are higher than those of AlP and NiP during the whole reaction time. Meanwhile, AlP shows higher acrolein selectivity and yield than NiP. The acrolein selectivity and yield of the samples are proportional to the B/L ratio rather than acid amount of sample. Higher value of B/L is more likely to produce acrolein. Similar results were reported by our and other groups previously [2,5,7,8].

As shown in Fig. 7, the catalytic performance of all the metal phosphate catalysts decreases in different degrees. After the glycerol dehydration reaction, a CHNS analyzer was used to determine the amount of carbon deposition during the reaction on the spent AlP, FeP and NiP. The results show that the coke content of the used AlP, FeP and NiP catalysts is approximately 1.1 wt%, 0.7 wt% and 3.7 wt%, respectively. The catalyst deactivation can be ascribed to carbon deposition on the catalyst surface blocking the active sites during the glycerol dehydration reaction.

CONCLUSIONS

Aluminium phosphate, iron phosphate and nickel phosphate catalysts were prepared using a simple replacement reaction method and evaluated for dehydration of glycerol to acrolein in a fixed bed reactor. The results showed that all metal phosphate catalysts remained in an amorphous state. The glycerol conversion was proportional to the acid amount of metal phosphate catalyst. A higher value of B/L was more likely to produce acrolein. After 2 h on stream, FeP was superior to the other metal phosphate catalysts due to its suitable textural and acid properties, with 96% glycerol conversion, 82% acrolein selectivity and 79% acrolein yield at 280 °C. The catalyst deactivation was ascribed to carbon deposition on the catalyst surface blocking the active sites during the reaction.

ACKNOWLEDGEMENTS

This work was supported by the University Natural Science Research Key Project of Anhui Province (KJ2018A0435, KJ2017A412), the University Natural Science Research General Project of Anhui

Province (KJ2018B15), Scientific Research Start Foundation Project of Chuzhou University (2017qd12, 2017qd15), and Anhui Provincial Natural Science Foundation (1808085MB50).

REFERENCES

1. A. Talebian-Kiakalaieh and N. A. S. Amin, *Renew. Energy*, **114**, 794 (2017).
2. M. Anitha, S. K. Kamarudin and N. T. Kofli, *Chem. Eng. J.*, **295**, 119 (2016).
3. P. Chagas, M. A. Thibau, S. Breder, P. P. Souza, G. S. Caldeira, M. F. Portilho, C. S. Castro and L. C. A. Oliveira, *Chem. Eng. J.*, **369**, 1102 (2019).
4. L. Shen, H. Yin, A. Wang, Y. Feng, Y. Shen, Z. Wu and T. Jiang, *Chem. Eng. J.*, **180**, 277 (2012).
5. T. Ma, Z. Yun, W. Xu, L. Chen, L. Li, J. Ding and R. Shao, *Chem. Eng. J.*, **294**, 343 (2016).
6. A. Talebian-Kiakalaieh, N. A. S. Amin and Z. Y. Zakaria, *J. Ind. Eng. Chem.*, **34**, 300 (2016).
7. T. Ma, J. Ding, R. Shao, W. Xu and Z. Yun, *Chem. Eng. J.*, **316**, 797 (2017).
8. J. Ding, T. Ma, M. Cui, R. Shao, R. Guan and P. Wang, *Mol. Catal.*, **461**, 1 (2018).
9. J. Ding, T. Ma, R. Shao, W. Xu, P. Wang, X. Song, R. Guan, K. Yeung and W. Han, *New. J. Chem.*, **42**, 14271 (2018).
10. J. Deleplanque, J. L. Dubois, J. F. Devaux and W. Ueda, *Catal. Today*, **157**, 351 (2010).
11. R. Estevez, S. Lopez-Pedrajas, F. Blanco-Bonilla, D. Luna and F. M. Bautista, *Chem. Eng. J.*, **282**, 179 (2015).
12. M. Akizuki, K. Sano and Y. Oshima, *J. Supercrit. Fluid*, **113**, 158 (2016).
13. K. H. Sung and S. Cheng, *RSC Adv.*, **7**, 41880 (2017).
14. A. Fernandes, M. F. Ribeiro and J. P. Lourenço, *Catal. Commun.*, **95**, 16 (2017).
15. C. D. Lago, H. P. Decolatti, L. G. Tonutti, B. O. D. Costa and C. A. Querini, *J. Catal.*, **366**, 16 (2018).
16. J. Shan, Z. Li, S. Zhu, H. Liu, J. Li, J. Wang and W. Fan, *Catalysts*, **9**, 121 (2019).
17. A. Talebian-Kiakalaieh and N. A. S. Amin, *Chinese J. Catal.*, **38**, 1697 (2017).
18. S. Lopez-Pedrajas, R. Estevez, R. Navarro, D. Luna and F. M. Bautista, *J. Mol. Catal. A: Chem.*, **421**, 92 (2016).
19. S. Lopez-Pedrajas, R. Estevez, F. Blanco-Bonilla, D. Luna and F. M. Bautista, *J. Chem. Technol. Biot.*, **92**, 2661 (2017).
20. Y. Li and C. Zhao, *Chem. Mater.*, **28**, 5659 (2016).
21. D. Fiorito, S. Folliet, Y. Liu and C. Mazet, *ACS Catal.*, **8**, 1392 (2018).
22. S. K. Lee, U. H. Lee, Y. K. Hwang, J. S. Chang and N. H. Jang, *Catal. Today*, **324**, 154 (2019).
23. C. A. Emeis, *J. Catal.*, **141**, 347 (1993).
24. B. Liu, P. Jiang, P. Zhang, H. Zhao and J. Huang, *C. R. Chim.*, **20**, 540 (2017).
25. H. Chai, H. Wang, Y. Liang and B. Xu, *J. Catal.*, **250**, 342 (2007).
26. M. M. Gadgil and S. K. Kulshreshtha, *J. Solid State Chem.*, **111**, 357 (1994).
27. A. Harilal, V. D. B. C. Dasireddy and H. B. Friedrich, *Catal. Lett.*, **146**, 1169 (2016).
28. S. Wu, P. Lai and Y. Lin, *Catal. Lett.*, **144**, 878 (2014).
29. W. Suprun, M. Lutecki, T. Haber and H. Papp, *J. Mol. Catal. A: Chem.*, **309**, 71 (2009).
30. D. Stošić, S. Bennici, S. Sirotin, C. Calais, J.-L. Couturier, J.-L. Dubois, A. Travert and A. Auroux, *Appl. Catal. A-Gen.*, **447**, 124 (2012).
31. E. Tsukuda, S. Sato, R. Takahashi and T. Sodesawa, *Catal. Commun.*, **8**, 1349 (2007).